Journal of Applied Polymer Science

Octakis(ethynyldimethylsiloxy) silsesquioxane: Synthesis and application in poly(silicane arylacetylene) resin

Xiaojun Bu, Yan Zhou, Chuan Li, Farong Huang
Key Laboratory for Specially Functional Polymeric Materials and Related Technology (East China University of Science and Technology), Ministry of Education, 130 Meilong Road, Shanghai 200237, China
Correspondence to: F. Huang (E-mail: fhuanglab@ecust.edu.cn)

ABSTRACT: Octakis(ethynyldimethylsiloxy)silsesquioxane (OEMS) was first synthesized via hydrolysis condensation reaction between tetramethylammonium octaanion and ethynyldimethylchlorosilane, and characterized by FT-IR, NMR, and GPC methods. A series of OEMS modified poly(silicane arylacetylene) resins (OEMS-PSAs) were prepared from OEMS and poly(silicane arylacetylene) (PSA). TEM analysis of the OEMS-PSAs confirms that the nano-sized polyhedral oligomeric silsesquioxanes (POSS) are dispersed evenly in low content, but aggregated unregularly in high content in OEMS-PSAs. The curing behavior of OEMS-PSAs was studied with DSC and FT-IR techniques. Nanoindentation test shows the incorporation of OEMS into PSA could decrease both of the elastic modulus and surface hardness of the PSA thermoset. The dielectric constants (ε_r) of the OEMS-PSA thermosets approach to 2.1, depending on not only the content of POSS but also the dispersion of POSS. Furthermore, TGA results demonstrate the OEMS-PSA thermosets possess the certain thermo-oxidative resistance. © 2016 Wiley Periodicals, Inc. J. Appl. Polym. Sci. **2016**, *133*, 44158.

KEYWORDS: high performance resins; nanoparticles; thermal properties; thermosets

Received 10 April 2016; accepted 3 July 2016
DOI: 10.1002/app.44158

INTRODUCTION

Poly(silicane arylacetylene) resin (PSA) composed of [–(R_1)Si(R_2)–C≡C-Ar-C≡C–] is a kind of high performance thermosetting resins.[1,2] PSA has already shown potential applications as ceramic precursors, heat-resistant materials, and matrices of advanced polymer composites in aerospace due to its excellent thermal properties. In addition, the dielectric constant of PSA thermoset is low ($\varepsilon_r < 3$), especially in high frequency range, suggesting the potential applications in high performance microelectronic devices.[3] Further modification of PSA is needed for the application in highly integrated circuit, because lower dielectric constant is beneficial to reduce the resistance capacitance time delay, cross-talks and power dissipation.[4] The incorporation of polyhedral oligomeric silsesquioxanes (POSS) into polymers is an effective way to reduce the ε_r of hybrid nanocomposites due to its nanoporosity.[3–6]

With a general structure of $(RSiO_{3/2})_8$, POSS has attracted much interest as a nanoscale building block for the construction of organic/inorganic hybrid materials.[7,8] POSS can be structurally well designed and easily functionalized with a wide variety of organic groups that are commonly used in polymerization or grafting reactions.[9,10] Researchers have found that dispersing POSS nanoparticles into a polymer can lead to enhancements in mechanical, thermal, and dielectric properties of the polymer.[11,12] The enhancements should be attributed to the "hybrid" characters of POSS from the chemical inertness and thermal stability of inorganic Si-O-Si core and the potentially reactive and readily modified Si-R groups.[13] Our previous investigations show that the incorporation of POSS structures into the well-established and high-performance PSA would likely to enhance resin properties and utility.[14–16] Zhou *et al.* made a series of PSAs containing octakis(dimethylsiloxy)octasilsesquioxane ($Q_8M_8^H$) by hydrosilylation reaction,[16] and the dielectric constants of the related thermosets decrease from 2.91 to 2.73, meanwhile the thermo-oxidative stabilities are obviously improved.

On the basis of $Q_8M_8^H$, here we have synthesized a novel ethynyl-terminated POSS, octakis(ethynyldimethylsiloxy)silsesquioxane (OEMS), as shown in Scheme 1. The novel OEMS is incorporated into PSA to produce OEMS-PSAs in this work. The structures and properties of the OEMS-PSAs are investigated.

EXPERIMENTAL

Materials

PSA was synthesized according to the method reported by Huang's group.[2] Tetramethylammonium octaanion and 1,3-dichloro-1,1,3,3-tetramethyldisiloxane were synthesized by

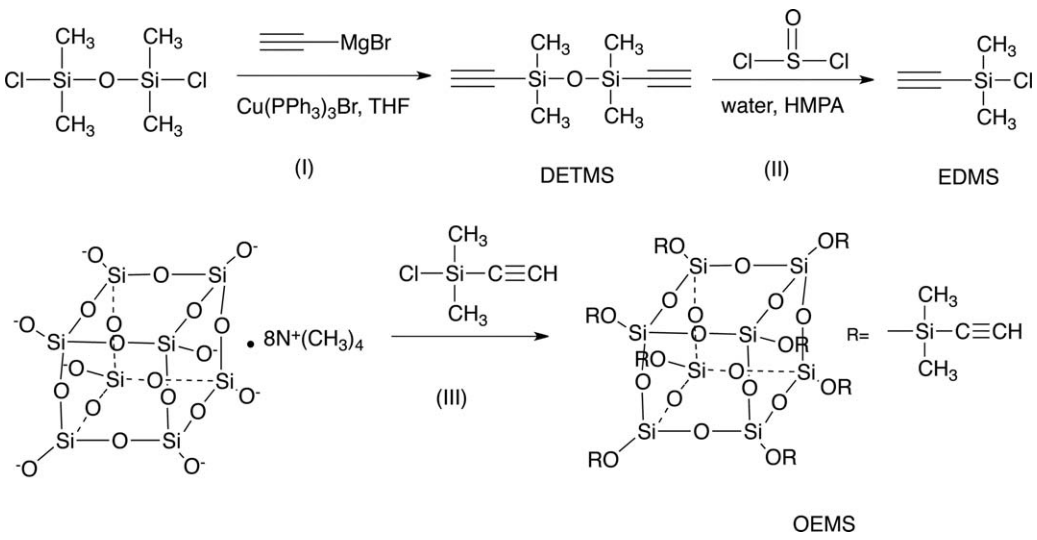

Scheme 1. Synthesis route of OEMS.

following literatures.[17,18] Ethynylmagnesium bromide was purchased from Aldrich Chemical (St. Louis, USA). Hexamethylphosphoramide (HMPA) was obtained from Adamas Reagent Co., Ltd (Shanghai, China). $Cu(PPh_3)_3Br$, pentane, thionyl chloride, hexane, DMSO, THF, and anhydrous sodium sulfate were purchased from Sinopharm Chemical Reagent (Shanghai, China). THF was dried over sodium filaments and distilled under N_2 before use.

Characterization

NMR spectra were recorded on a Bruker Avance 400 NMR spectrometer (400 MHz, Bruker, Switzerland) at room temperature in $CDCl_3$ (0.05% TMS as an internal standard). Molecular weight distribution was analyzed on a GPC instrument equipped with a Waters 515 HPLC pump (Waters, Massachusetts, USA). THF served as an eluent at a flow rate of 1 mL min^{-1}. Differential scanning calorimetric (DSC) analyses were recorded with a TA Q2000 instrument (TA Instruments, USA) at a scanning rate of 10 °C min^{-1} under nitrogen flow (50 mL min^{-1}). The hardness and elastic modulus measurements were estimated with the Oliver-Pharr method in the nanoindentation testing with a G200 Nano Indenter (Agilent Technologies, USA): a diamond pyramid Berkovich identer with a tip radius of about 20 nm and face angle of 65.3° was used. The Poisson's ratio of the sample was estimated as 0.3. The indentation tests were run in a load-control mode, using a maximum indentation load of 100 mN. During the test, the loading speed was kept as a constant force increasing as 10 mN s^{-1} for 10 s. The peak-hold time, that is, the time the indenter held at the maximum load, was set as 10 s. Indentation tests for each sample were repeated five times, and each test point was at least 5 μm apart to avoid interactions between the stress fields of the neighboring indentations. Dielectric property measurements were carried out on a Concept 40 (Novocontrol, Germany) in the range of measuring frequency from 10^1 to 10^6 Hz at room temperature. The thermal stabilities of the cured resins were measured by TGA/DSC 1 thermogravimetric analyzer (Mettler-Toledo, Switzerland) in the range between room temperature and 800 °C at a heating rate of 10 °C min^{-1} under an air purge with a flux of 80 mL min^{-1}. About 5 mg samples were weighed into ceramic crucibles for the measurements.

Synthesis of 1,3-Diethynyl-1,1,3,3-Tetramethyldisiloxane (DETMS)

1,3-Diethynyl-1,1,3,3-tetramethyldisiloxane (DETMS) was synthesized according to the reference.[19] 20.0 g 1,3-Dichloro-1,1,3,3-tetramethyldisiloxane (100 mmol), 0.2 g $Cu(PPh_3)_3Br$ (0.2 mmol), and 100 mL dry THF were charged into a round-bottom flask, to which 400 mL THF solution of ethynylmagnesium bromide (0.6 *M*) was quickly added under nitrogen at room temperature. The mixture was magnetically stirred for 4 h at 66 °C, followed by the removal of THF on a rotary evaporator. The resulting mixture was extracted using pentane as a solvent. The combined pentane solution was concentrated with a rotary evaporator, and then distillated to give DETMS as a colorless liquid (b.p.: 125 °C, yield: 56%). ^1H NMR (400 MHz, $CDCl_3$, δ): 0.3 (m, 6H, —CH_3), 2.4 (s, H, ≡CH).

Synthesis of Ethynyldimethylchlorosilane (EDMS)

Yameen[19] reported a route to prepare ethynyldimethylchlorosilane (EDMS) using methyltrichlorosilane as a chlorinating agent. From the standpoint of easily hydrolytic property and low boiling point, we replaced methyltrichlorosilane with thionyl chloride to synthesize EDMS. In a 20 mL round-bottom flask, a mixture of 3.0 g DETMS (16.5 mmol), 5.6 g thionyl chloride (46.8 mmol), 0.2 μL HMPA, and 12 μL deionized water was stirred in N_2 at 60 °C for 1 h. The reaction mixture was then distillated to give EDMS as a colorless liquid in the yield of 80% (b.p.: 40 °C). ^1H NMR (400 MHz, $CDCl_3$, δ): 0.3 (m, 6H, –CH_3), 2.4 (s, H, ≡CH).

Synthesis of OEMS

A solution of 0.19 g EDMS (1.6 mmol) in 10 mL hexane and 10 mL DMSO was charged into a round-bottom flask, to which 0.11 g tetramethylammonium octaanion (0.1 mmol) was added in batches at 0 °C under nitrogen. The mixture was warmed up to room temperature and magnetically stirred for 4 h. The hexane phase was separated, washed with deionized water, and then dried over anhydrous Na_2SO_4. Finally, the hexane solution

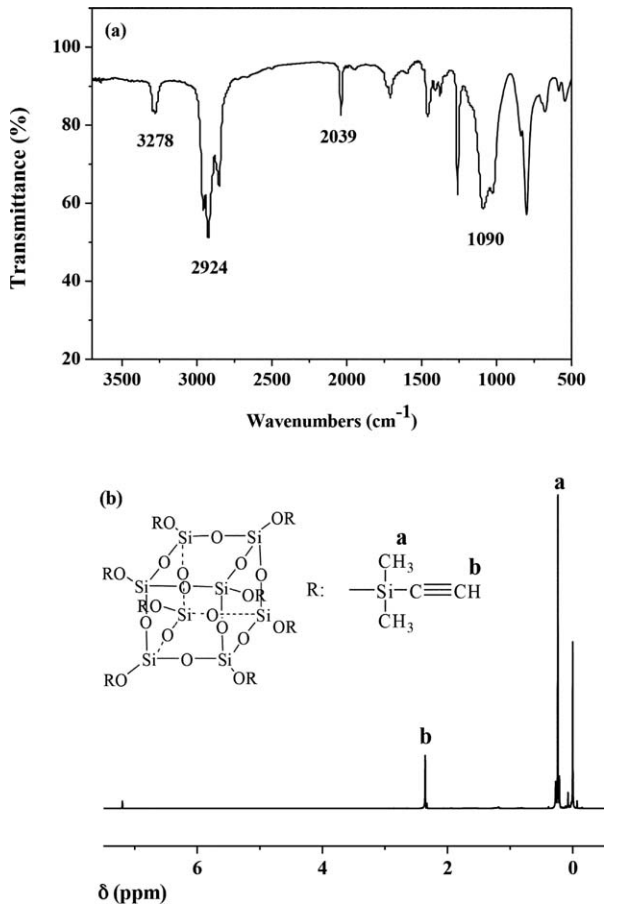

Figure 1. The FT-IR (a) and ^{1}H-NMR (b) spectra of OEMS.

was evaporated on a rotary evaporator to give OEMS as a white solid (yield: 60%). GPC (polystyrene calibration): $M_n = 1208$ g mol^{-1}, $D = 1.02$; FTIR (KBr): 1090 (s; ν_s(SiOSi)), 2039 (ms; β(C≡C)), 2924 (s; ν_s(C-H)), 3278 (ms; ν_s(≡CH)); ^{1}H NMR (400 MHz, $CDCl_3$, δ): 0.3 (m, 6H, –CH_3), 2.4 (s, H, ≡CH); ^{29}Si NMR (400 MHz, $CDCl_3$, δ): −21.87 (Si); Anal. calcd for $Si_{16}O_{20}C_{32}H_{56}$: C 31.79, H 4.63; found: C 31.33, H 4.39.

Preparation of OEMS-PSAs and Thermosets

OEMS was incorporated into the PSA with 1, 3, 5, and 10% in weight ratios. Appropriate quantities of OEMS, PSA, and THF were charged into a flask and the mixture was kept stirring till a homogenous liquid was obtained. THF was removed by a rotary evaporator at 40 °C, and then, the light yellow resin was dried in vacuum. The relative OEMS-PSAs obtained were named as OEMS-PSA-1, OEMS-PSA-3, OEMS-PSA-5, and OEMS-PSA-10. The corresponding dark-brown, hard, and dense thermosets were obtained after the following curing process: 150 °C for 2 h, 170 °C for 2 h, 210 °C for 2 h, and 250 °C for 4 h. The OEMS-PSA thermosets were named as OEMS-PSA-1C, OEMS-PSA-3C, OEMS-PSA-5C, and OEMS-PSA-10C, respectively.

RESULTS AND DISCUSSION

Synthesis and Characterization of OEMS

Figure 1 shows the FT-IR and ^{1}H-NMR spectra of the OEMS. In Figure 1(a), the band at 1090 cm^{-1} is a strong Si-O-Si stretching absorption for silsesquioxane cages.[20,21] The C≡C out-of plane bending vibration at 2039 cm^{-1} and the ≡C-H stretching vibration at 3278 cm^{-1} belong to the characteristic absorptions of the ethynyl groups.[22,23] The C-H asymmetric stretching vibration of CH_3 is at 2924 cm^{-1}.[24,25] In Figure 1(b), the signals of resonance at 0.3 ppm are assignable to methyl protons, and the signal of resonance appearing at 2.4 ppm corresponds to the ethynyl proton.[19]

Morphology of OEMS-PSAs

The dispersion of OEMS in PSA is observed via TEM. At the low content of 3% OEMS, the well-dispersed nanoparticles with a relatively uniform diameter of about 30 nm are observed [Figure 2(a)]. The size of nanoparticles increases to about 100 nm as the OEMS content increases to 5% [Figure 2(b)]. With further increasing the content of OEMS to 10%, a different assembled morphology is observed, as shown in Figure 2(c). There are both spherical nanoparticles and some irregular aggregates, and the distribution of these aggregates is nonhomogeneous. POSS with an inorganic and silica-like core surrounded by eight organic groups has an overwhelming tendency to aggregate in polymer, resulting to a phase-segregated structure.[26–28] TEM images indicate that a good dispersion can be achieved at a low content of OEMS. However, the irregular POSS aggregates occur with a high content of OEMS.

Curing Behavior of OEMS-PSAs

DSC measurement results are shown in Figure 3. The corresponding T_i (initial curing temperature) and T_p (curing peak temperature) are listed in Table I. As shown in the table, the T_p's of OEMS and PSA are 279.1 °C and 238.4 °C, respectively. For the OEMS-PSAs, all the DSC thermograms display single exothermal peak in the temperature range from 241.0 °C to 251.7 °C, and the T_p increases with the OEMS content increasing from 0 to 10%. The endothermic peaks around 100 °C in the thermograms of OEMS-PSAs are attributed to the melting

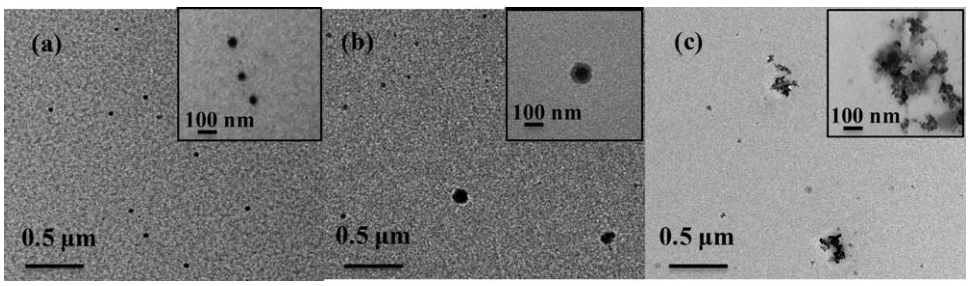

Figure 2. TEM micrographs of OEMS-PSA-3 (a), OEMS-PSA-5 (b), and OEMS-PSA-10 (c).

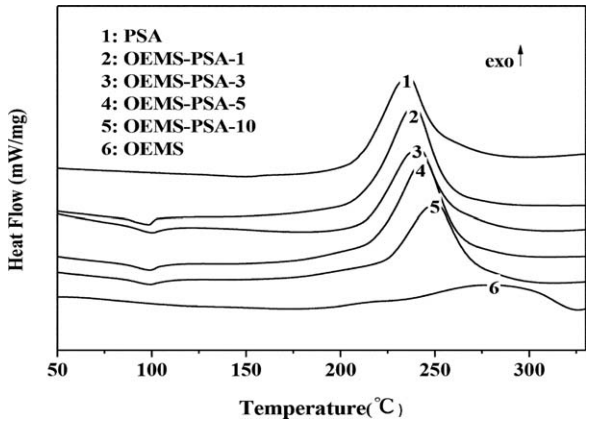

Figure 3. DSC curves of OEMS-PSAs.

behavior of the resins. That indicates there is significant influence of OEMS on the crystallinity of PSA.

Figure 4 shows the FT-IR spectra of OEMS, OEMS-PSA-5, and OEMS-PSA-5C. It is obvious that the absorption peaks at 2030 cm^{-1} (C≡C) and 3290 cm^{-1} (≡C—H) of OEMS is considerably weaken but still exist after curing, indicating the incompletely reaction of ethynyl moieties on OEMS.

DSC measurements in the range of 125–350 °C at the heating rates of 5, 10, 15, and 20 °C min^{-1} are conducted to investigate the curing kinetics of PSA and OEMS-PSA-5 (Figure 5). For both PSA and OEMS-PSA-5, the curing exothermal peaks shift to a high temperature region as the heating rate increases. Based on the Flynn/Wall/Ozawa method,[29] the DSC analysis data are treated and analyzed.

The extent of conversion α_T at a certain temperature T is calculated on the exothermal heat ΔH as:

$$\alpha_T = \frac{\Delta H_T}{\Delta H} \quad (1)$$

The empirical equation described by Sastri[29] can be used to evaluate the apparent activation energy (E_α):

$$E_\alpha = \frac{-R}{0.4567}\frac{\Delta \ln \beta}{\Delta(1/T_\alpha)} \quad (2)$$

T_α is the temperature at which a given conversion α is reached with the heating rate. As shown in Figure 6, the data obtained

Table I. DSC Analysis Results of OEMS-PSA Resins

Samples	T_i (°C)	T_p (°C)	Exothermal heat (J/g)
PSA	212	238	473
OEMS-PSA-1	213	241	411
OEMS-PSA-3	214	242	395
OEMS-PSA-5	216	244	359
OEMS-PSA-10	220	252	330
OEMS	217	279	158

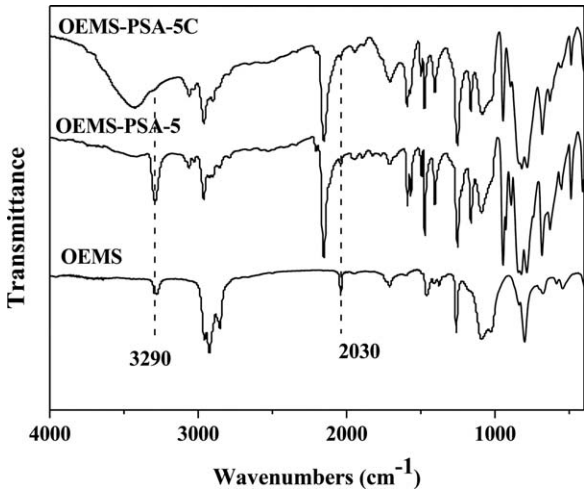

Figure 4. FT-IR spectra of OEMS, OEMS-PSA-5, and OEMS-PSA-5C.

from the thermograms is a straight line (linear correlation coefficients: 0.92–0.98). The E_α's are estimated from the slope of the lines and listed in Table II.

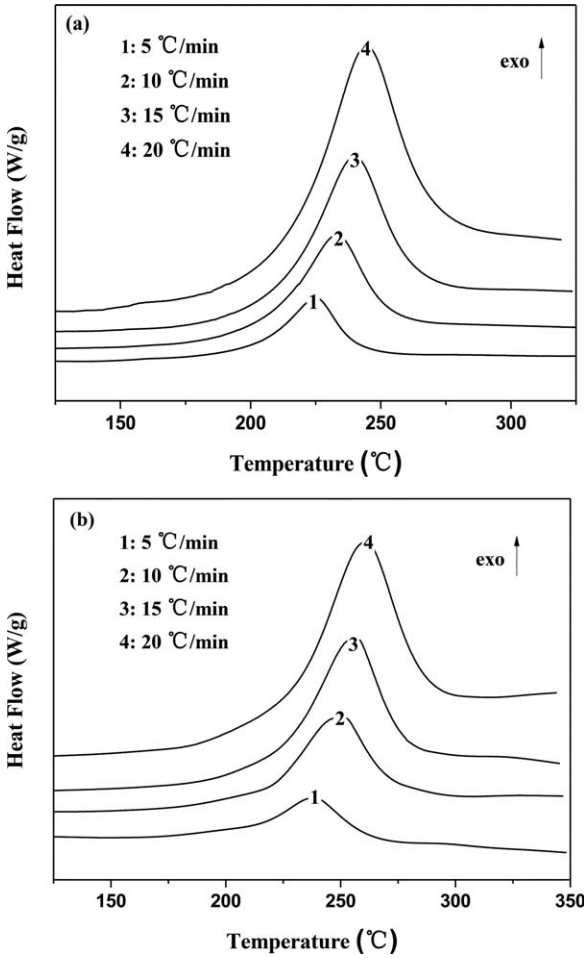

Figure 5. DSC curves of PSA (a) and OEMS-PSA-5 (b) at various heating rates.

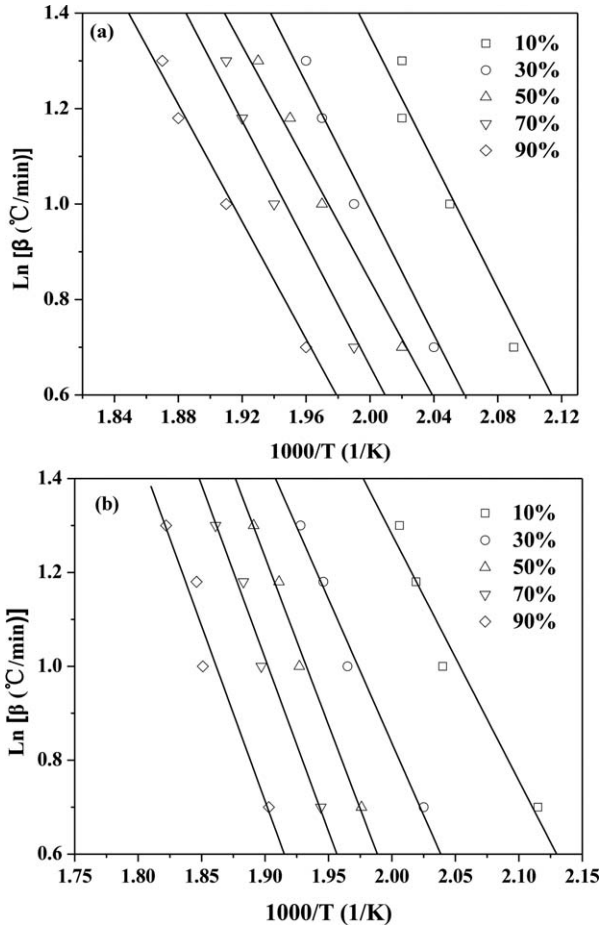

Figure 6. The plots of ln β versus 1/T for PSA (a) and OEMS-PSA-5 (b).

The Diels–Alder reaction, trimerization and radical polymerization between ethynyls and ethynylenes are reported to be the major crosslinking reaction for PSA.[30] In the crosslinking system, crosslinking density is mainly determined by the mole content of the ethynyls. The molar ratio of ethynyls (excluding ethynylene group) in OEMS and PSA is 1.75:1 based on the equivalent mass of OEMS and PSA. The incorporation of OEMS increases the content of ethynyls in OEMS-PSAs. As shown in Table II, when α is 10%, E_α for OEMS-PSA-5 is about 95 KJ mol^{-1} which is lower than 112 KJ mol^{-1} for PSA. It indicates the curing reaction is easy to occur with the incorporating of OEMS. E_α for OEMS-PSA-5 increases gradually with increment in α throughout the curing process. High E_α means the mobility of the reactive ethynyls decreases.[31] Therefore, some of the ethynyls could not diffuse and react fast, and are finally trapped in an unreacted form in the cured OEMS-PSA-5, which corresponds to the presence of the ethynyls in the FT-IR spectra in Figure 4.

Table II. Non-Isothermal Apparent Curing Activation Energy of PSA and OEMS-PSA-5

	The extent of conversion α (%)				
E_α (kJ/mol)	10	30	50	70	90
PSA	112	114	112	120	120
OEMS-PSA-5	95	112	130	134	135

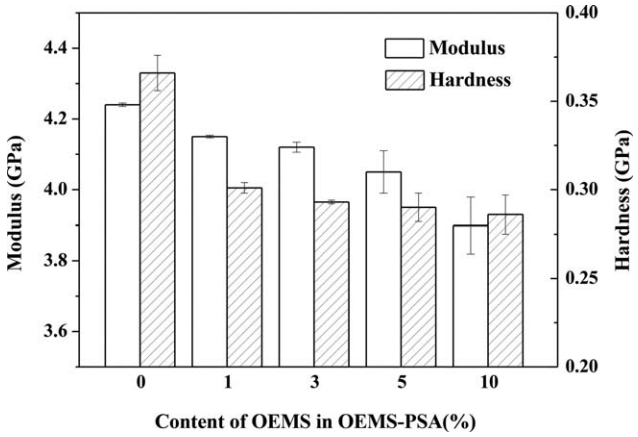

Figure 7. Modulus and hardness of PSA and OEMS-PSA thermosets measured by nanoindentation.

Nanoindentation of OEMS-PSA Thermosets

Figure 7 presents the elastic modulus and hardness of PSA and OEMS-PSA thermosets measured by nanoindenter with a Berkowich diamond tip. A modest change in elastic modulus and hardness is observed as the loading of OEMS increases. The elastic modulus and surface hardness of PSA thermoset is 4.2 and 0.37 GPa, respectively. For OEMS-PSA-10C, the modulus and hardness exhibit the reduction of 8 and 22%, respectively. The reductions in the modulus and hardness indicate the decrease in rigidity of the thermosets, which is related to components of the thermosets and the crosslinked structures. As mentioned above, not all the ethynyls in OEMS-PSAs participate in the curing reaction. Furthermore, the addition of OEMS leads to the crosslinked structures different from PSA thermoset. The low modulus and hardness would probably be ascribed to the variation in the components and crosslinked structures of the thermosets.[32]

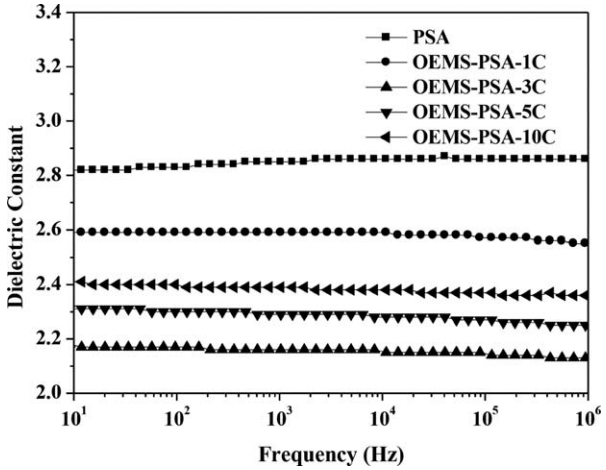

Figure 8. Frequency dependence of dielectric constant for PSA and OEMS-PSA thermosets.

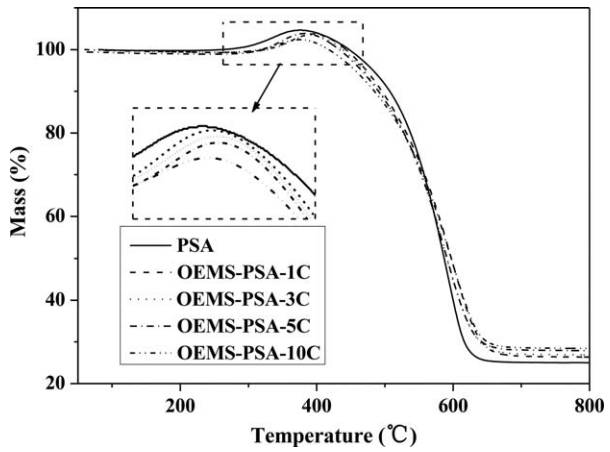

Figure 9. TGA thermograms of OEMS-PSA thermosets in air.

Dielectric Properties of OEMS-PSA Thermosets

The frequency dependence of dielectric constants (ε_r) for OEMS-PSA thermosets at the frequency range from 10 Hz to 1 MHz is shown in Figure 8. It can be seen that ε_r is very weakly dependent on frequency, which is the typical characteristic of non-polar polymers. PSA thermoset exhibits ε_r of 2.81–2.85. The ε_r of OEMS-PSA thermosets first decreases and then increases with the OEMS content increasing. The OEMS-PSA thermosets possess significantly lower ε_r than that of PSA, demonstrating that incorporating of OEMS into PSA can effectively reduce the ε_r. The maximum reduction in the dielectric constant is about 24% ($\varepsilon_r = 2.1$) for OEMS-PSA-3C as compared with PSA thermoset. The values are much lower than that of the Q_8M_8 modified PSA thermosets ($\varepsilon_r = 2.7$).[16] The low ε_r, especially in high frequency, implies the potential application of OEMS-PSA thermosets in high performance microelectronic devices.

The reduction of ε_r is mainly due to the increment in the free volume[33,34] because of the POSS core and the external porosity introduced by tethering OEMS to the PSA. Ke *et al.*[35] reported that the contribution of the intrinsic POSS core to the increased free volume is very small compared with the total increased free volume, whereas the steric hindrance of the external porosity plays a dominant role in the growth of free volume and thus reduction of low dielectric constant. A high content of OEMS in OEMS-PSA thermosets produces an aggregation and the formation of the aggregation could lead to the reduction of the external porosity, which results in a high ε_r.

Thermo-Oxidative Stability of OEMS-PSA Thermosets

The thermo-oxidative behavior of OEMS-PSA thermosets is analyzed with TGA under air atmosphere, as shown in Figure 9. The characteristic mass loss temperatures and mass residues for OEMS-PSA thermosets are presented in Table III. A weight increment as the evidence of oxidation is observed on heating the thermosets and occurs approximately at 300 °C. PSA thermoset gains a maximum weight of 4.7% around 400 °C while this weight increment of OEMS-PSA thermosets decreases gradually to 2.4% with the content of OEMS increasing. This indicates that OEMS-PSA thermosets present better resistance to thermo-oxidative than PSA thermoset. The T_{d5} (temperatures at 5% weight loss) of OEMS-PSA thermosets decreases continuously with the increase in OEMS content. However, the characteristic T_{d50} (temperatures at 50% weight loss) increases with the incorporation of OEMS. The decrease of the mass loss rate indicates an increment of thermo-oxidative stability. It is probably attributed to the formation of a silica layer on the surface of the thermosets to prevent further degradation of the underlying thermosets.[36] The thermo-oxidative stability of OEMS-PSA thermosets is also observed in the increased residue yield at 800 °C.

Table III. Thermal Oxidative Decomposition of OEMS-PSA Thermosets by TGA under Air

Contents of OEMS (%)	0	1	3	5	10
T_{d5} (°C)	483	472	469	466	456
T_{d50} (°C)	587	589	591	592	597
Residue at 800 °C (%)	25.0	26.3	26.9	28.5	28.4

CONCLUSIONS

A novel OEMS was synthesized and used to modify PSA in different weight ratios. By changing the weight ratios, the existence of POSS nanoparticles as well as POSS aggregates can be achieved. The curing reaction investigations show that incorporating of OEMS leads to variable apparent activation energy (from 95 to 135 kJ mol^{-1}) and the ethynyls on OEMS react incompletely at the temperature lower than 250 °C. After the curing process, OEMS-PSA thermosets present decreased modulus and hardness compared to PSA thermoset. The dielectric constant (ε_r) of OEMS-PSA thermoset depends on the content of OEMS and achieves as low as 2.1. The OEMS-PSA thermosets show a high T_{d5} above 450 °C in air, and offer additional advantages of certain thermal oxidative resistance. The OEMS-PSA thermosets with low dielectric constant and high temperature oxidation resistance would be expected in the potential application on high performance microelectronic devices.

REFERENCES

1. Wang, F.; Zhang, J.; Huang, J.; Yan, H.; Huang, F.; Du, L. *Polym. Bull.* **2005**, *56*, 19.
2. Gao, F.; Zhang, L.; Tang, L.; Zhang, J.; Zhou, Y.; Huang, F.; Du, L. *Bull. Korean Chem. Soc.* **2010**, *31*, 976.
3. Vengatesan, M. R.; Devaraju, S.; Dinakaran, K.; Alagar, M. *J. Mater. Chem.* **2012**, *22*, 7559.
4. Geng, Z.; Huo, M.; Mu, J.; Zhang, S.; Lu, Y.; Luan, J.; Huo, P.; Du, Y.; Wang, G. *J. Mater. Chem. C* **2014**, *2*, 1094.
5. Liao, W. H.; Yang, S. Y.; Hsiao, S. T.; Wang, Y. S.; Li, S. M.; Ma, C. C.; Tien, H. W.; Zeng, S. J. *ACS Appl. Mater. Interfaces* **2014**, *6*, 15802.
6. Su, R. Q.; Muller, T. E.; Prochazka, J.; Lercher, J. A. *Adv. Mater.* **2002**, *14*, 1369.
7. Markovic, E.; Constantopolous, K.; Matisons, J. G. *Cheminform* **2011**, *44*, 1.
8. Wang, F.; Lu, X.; He, C. *J. Mater. Chem.* **2011**, *21*, 2775.

9. Chimjarn, S.; Kunthom, R.; Chancharone, P.; Sodkhomkhum, R.; Sangtrirutnugul, P.; Ervithayasuporn, V. *Dalton Trans.* **2015**, *44*, 916.
10. Żak, P.; Majchrzak, M.; Wilkowski, G.; Dudziec, B.; Dutkiewicz, M.; Marciniec, B. *RSC Adv.* **2016**, *6*, 10054.
11. Roy, S.; Lee, B. J.; Kakish, Z. M.; Jana, S. C. *Macromolecules* **2012**, *45*, 2420.
12. Qing, R.; Muller, T. E.; Prochazka, J.; Lercher, J. A. *Adv. Mater.* **2002**, *19*, 1369.
13. Cordes, D. B.; Lickiss, P. D.; Rataboul, F. *Chem. Rev.* **2010**, *110*, 2081.
14. Jiang, Z.; Zhou, Y.; Huang, F.; Du, L. *Chin. J. Polym. Sci.* **2011**, *29*, 726.
15. Bu, X.; Zhou, Y.; Huang, F. *Mater. Lett.* **2016**, *174*, 21.
16. Zhou, Y.; Huang, F.; Du, L.; Liang, G. *Polym. Eng. Sci.* **2014**, *55*, 316.
17. Ishikawa, M.; Toyoda, E.; Ishii, M.; Kunai, A.; Yamamoto, Y.; Yamamoto, M. *Organometallics* **1994**, *13*, 808.
18. Carmo, D. R. D.; Guinesi, L. S.; Filho, N. L. D.; Stradiotto, N. R. *Appl. Surf. Sci.* **2004**, *235*, 449.
19. Yameen, B.; Ali, M.; Álvarez, M.; Neumann, R.; Ensinger, W.; Knoll, W.; Azzaroni, O. *Polym. Chem.* **2010**, *1*, 183.
20. Niu, M.; Li, T.; Xu, R.; Gu, X.; Yu, D.; Wu, Y. *J. Appl. Polym. Sci.* **2013**, *129*, 1833.
21. Zhang, W.; Müller, A. H. E. *Macromolecules* **2010**, *43*, 3148.
22. Gao, F.; Zhang, L.; Zhou, Y.; Huang, F.; Du, L. *J. Macromol. Sci. Part A* **2010**, *47*, 861.
23. Shen, Y.; Yuan, Q.; Huang, F.; Du, L. *Thermochim. Acta* **2014**, *590*, 66.
24. Wang, C.; Jiang, Y.; Gao, Y.; Zhou, Y.; Huang, F.; Du, L. *Polym. Eng. Sci.* **2012**, *52*, 1301.
25. Yang, Y.; Chen, G.; Liew, K. M. *J. Appl. Polym. Sci.* **2009**, *114*, 2706.
26. Frank, K. L.; Exley, S. E.; Thornell, T. L.; Morgan, S. E.; Wiggins, J. S. *Polymer* **2012**, *53*, 4643.
27. Zhang, D.; Liu, Y.; Shi, Y.; Huang, G. *RSC Adv.* **2014**, *4*, 6275.
28. Herman Teo, J. K.; Toh, C. L.; Lu, X. *Polymer* **2011**, *52*, 1975.
29. Sastri, S. B.; Keller, T. M.; Jones, K. M.; Armistead, J. P. *Macromolecules* **1993**, *26*, 6171.
30. Zhang, J.; Huang, J.; Du, W.; Huang, F.; Du, L. *Polym. Degrad. Stab.* **2011**, *96*, 2276.
31. Kim, G. M.; Qin, H.; Fang, X.; Sun, F. C.; Mather, P. T. *J. Polym. Sci. Part B* **2003**, *41*, 3299.
32. Huang, J.; He, C.; Liu, X.; Xu, J.; Tay, C. S. S.; Chow, S. Y. *Polymer* **2005**, *46*, 7018.
33. Leu, C. M.; Chang, Y. T.; Wei, K. H. *Macromolecules* **2003**, *36*, 9122.
34. Leu, C. M.; Reddy, G. M.; Wei, K. H.; Shu, C. F. *Chem. Mater.* **2003**, *15*, 2261.
35. Ke, F.; Zhang, C.; Guang, S.; Xu, H. *J. Appl. Polym. Sci.* **2013**, *127*, 2628.
36. Zheng, L.; Kasi, R. M.; Farris, R. J.; Coughlin, E. B. *J. Polym. Sci. Part A* **2002**, *40*, 885.